

Effect of Heating Rate on the Slow Pyrolysis Behaviour and Its Kinetic Parameters of Oil-Palm Shell

Fredy Surahmanto^{*‡}, Harwin Saptoadi^{*}, Hary Sulistyono^{**}, Tri Agung Rohmat^{*}

^{*}Department of Mechanical and Industrial Engineering, Faculty of Engineering, Universitas Gadjah Mada, Indonesia

^{**}Department of Chemical Engineering, Faculty of Engineering, Universitas Gadjah Mada, Indonesia

(fredy.surahmanto@mail.ugm.ac.id, harwins@ugm.ac.id, hary@ugm.ac.id, triagung_rohmat@ugm.ac.id)

[‡] Corresponding Author: Fredy Surahmanto, Department of Mechanical and Industrial Engineering, Faculty of Engineering, Universitas Gadjah Mada, Yogyakarta, Postal code: 55281, Indonesia; Tel: +62 82211357345, fredy.surahmanto@mail.ugm.ac.id

Received: 06.01.2017 Accepted: 05.03.2017

Abstract - The effect of heating rate on the slow pyrolysis behaviour and its kinetic parameters was investigated in this study. Pyrolysis experiment with oil-palm shell waste as raw material was conducted in nitrogen atmosphere at heating rates of 5, 10, 15, and 20 °C /minute and final temperature of 550 °C by a simultaneous thermogravimetric analyser. The results show that heating rate affects the thermogravimetric curve position, maximum decomposition rate, and the temperature on which the maximum mass loss rate occur. Moreover, it can be known that calculated activation energies and frequency factors vary, depend on the specified temperature range and reaction order. By approximating the pyrolysis stages into four temperature ranges for reaction order of one and into five ones for reaction order of two and three, it was obtained that the activation energy values are from 6.90 to 203.10 kJ/mol and frequency factor values range from 1.283E-01 to 7.07E+15 s⁻¹.

Keywords – pyrolysis, kinetic, oil-palm shell, activation energy, frequency factor

1. Introduction

In recent times, pressures on the global environment have been demanding the use of renewable energy sources [1]. Biomass is one of the most common forms that is widely used due to its abundant availability in agricultural and plantation residues [2], [3]. In this case, the oil-palm (*Elaeis guineensis* Jacq.) could be an appropriate choice due to its intensive development for palm-oil production.

The oil palm grows well in wet-tropical plains, lay along equator region, between 10° N and 10° S of three continents. The historical and fossil evidence suggests that it was originally planted in West before being spread over in Africa, East Asia, and America [4]. At the present time, large scales of oil-palm plantations have been intentionally expanded for palm-oil production by extracting the flesh part and the innermost nut of the palm fruit. Based on the data from Foreign Agriculture Service, United States Department of Agriculture (2007), it can be known that world's oil-palm production in 2006 was very great in quantity, as 36.845 mega tons, in which Indonesia and Malaysia had the most

contribution, each gave 15.9 mega tons and 15.881 mega tons, respectively, followed by Thailand, Nigeria, Columbia, each gave 0.82; 0.815; 0.711 mega tons, respectively and the rest of 2.718 mega tons from other countries [5]. That production from Indonesia and Malaysia has been increasing during this last decade and is being predicted to be continuously increasing for the upcoming years.

As a consequence from the production increase, the quantity of oil-palm solid wastes, including shell, fibre and kernel will certainly be abundant. For every ton of palm oil produced from fresh fruit bunches, approximately one ton of empty fruit bunch, 0.7 ton of palm fibres, 0.3 ton of palm kernels and 0.3 ton of palm shells are remained [6]. By this approximation, it can be estimated that the total biomass generated from the palm oil industry would be around 84.74 mega tons. To prevent environmental threats, of course, proper handling is needed for this large amount of biomass. So, these renewable energy materials could be used as alternatives for producing valuable chemical-products by applying thermochemical conversion processes, including pyrolysis, combustion, gasification [7]–[12].

Pyrolysis is a promising process for biomass upgrading by cracking polymer structure of lignocellulosic materials and converting it into volatile fraction consisting of gases, vapours, tar components and char [13]–[15]. The knowledge and understanding on pyrolysis kinetics of biomass are needed to properly design and establish efficient and safe process [16]–[19].

Pyrolysis kinetics have been studied by means of several technologies, however, thermogravimetric analysis is the technique generally used, and regarded as a referential technique for accessing the thermal degradation behaviour of solid materials [20], [21]. In this technique, the change of sample mass is monitored against time or temperature in the absence of oxygen at specified heating rate. This technique has been widely applied for utilizing biomass wastes such as: microalgae [13], mosso bamboo [22], hazelnut husk [23], sugarcane baggase and cotton stalk [16], olive oil pomace [24], wood [14], [21], date palm [25], wheat straw [19], corn stover [26]. There have been various studies on pyrolysis analysis of different biomasses but their properties can significantly affect both heat transfer and reaction rates so that the operating conditions will be highly variable [27].

Although there are many studies on biomass pyrolysis using thermogravimetric analysis, however, that study on oil-palm shell is still limited. Therefore, this research aimed at investigating slow pyrolysis behaviour of oil-palm shell and its kinetic parameters in various heating rates.

2. Methods

2.1. Material and experiment

Oil-palm shell samples used in this study were obtained from a palm-oil mill. Prior to thermogravimetric experiments, oil-palm shells were previously crushed into small fractions and then sieved into size of 0.21 mm. Proximate and ultimate analysis were carried out to characterize these samples. The results are shown in Table 1.

Table 1. Proximate and ultimate analysis of oil-palm shell.

Proximate analysis (wt. %)	
Moisture	7.63
Volatile matter	63.36
Ash	1.04
Fixed carbon	27.98
Calorific value (cal/g)	4781.01
Ultimate analysis (wt. %, dry basis)	
Carbon	49.01
Hydrogen	6.18
Nitrogen	0.27
Sulphur	0.04
Oxygen	43.46

Pyrolysis tests were conducted by an automatic simultaneous thermal analyser, which provides simultaneous thermogravimetry (TG) and differential thermal analysis (DTA) on a single sample (Shimadzu, DTG – 60, Japan; with

temperature accuracy of 0.1 K, DTA sensitivity of 0.1 μ V and TG sensitivity of 1 μ g). For every run, about 8 mg sample was used and 15 ml/minute nitrogen was flowed to provide an inert atmosphere. Heating rate variation of 5, 10, 15, 20 $^{\circ}$ C/minute were applied and initial temperature of 30 $^{\circ}$ C, final temperature of 550 $^{\circ}$ C, and then holding time for 20 minutes were set. The instrument provided continuous recording of TG and DTA curves and data that were used to calculate the kinetic parameters. Each experiment was repeated at least twice to ensure its reproducibility.

2.2. Kinetics theory

Non-isothermal solid decomposition rate, is mathematically expressed as:

$$\frac{d\alpha}{dt} = kf(\alpha) \quad (1)$$

where α is flammable material conversion which is defined as:

$$\alpha = \frac{m_i - m_t}{m_i - m_f} \quad (2)$$

where m_t , m_i , and m_f represent instanteneous, initial and final mass of sample.

Reaction rate constant, k , is expressed by Arrhenius equation terms:

$$k(T) = Ae^{\left(\frac{-E}{RT}\right)} \quad (3)$$

Function $f(\alpha)$ can be written as:

$$f(\alpha) = (1 - \alpha)^n \quad (4)$$

where n is a reaction order.

Substitution of eq.(3) and eq.(4) into eq.(1), results in:

$$\frac{d\alpha}{dt} = Ae^{-E/RT} (1 - \alpha)^n \quad (5)$$

By using constant heating rate, $\beta = \frac{dT}{dt}$, eq.(5) can be arranged as:

$$\frac{d\alpha}{dT} = \frac{A}{\beta} e^{-E/RT} (1 - \alpha)^n \quad (6)$$

Solution of Eq.(6) results in:

$$\ln \left[\frac{-\ln(1-\alpha)}{T^2} \right] = \ln \left[\frac{AR}{\beta E} \left(1 - \frac{2RT}{E} \right) \right] - \frac{E}{RT}; \quad \text{if } n = 1 \quad (7)$$

$$\ln \left[\frac{1 - (1-\alpha)^{1-n}}{(1-n)T^2} \right] = \ln \left[\frac{AR}{\beta E} \left(1 - \frac{2RT}{E} \right) \right] - \frac{E}{RT}; \quad \text{if } n \neq 1 \quad (8)$$

Using asymptotic approximation, where $2RT/E \ll 1$, so $\ln \left[\frac{AR}{\beta E} \left(1 - \frac{2RT}{E} \right) \right] \approx \ln \left[\frac{AR}{\beta E} \right]$. Both plot $\ln \left[\frac{-\ln(1-\alpha)}{T^2} \right]$

versus $1/T$ for $n = 1$ and plot $\ln \left[\frac{1 - (1-\alpha)^{1-n}}{(1-n)T^2} \right]$ versus $1/T$ for

$n \neq 1$ will give linear curves. Activation energy, E and frequency factor, A can be determined by the slope and the intercept of the regression line.

3. Results and Discussion

3.1 Thermogravimetry analysis

Thermogravimetric experiment results at heating rate of 5, 10, 15, and 20 °C/minute are illustrated in thermogravimetric (TG) and derivative thermogravimetric (DTG) curves as shown in Fig. 1 and Fig. 2.

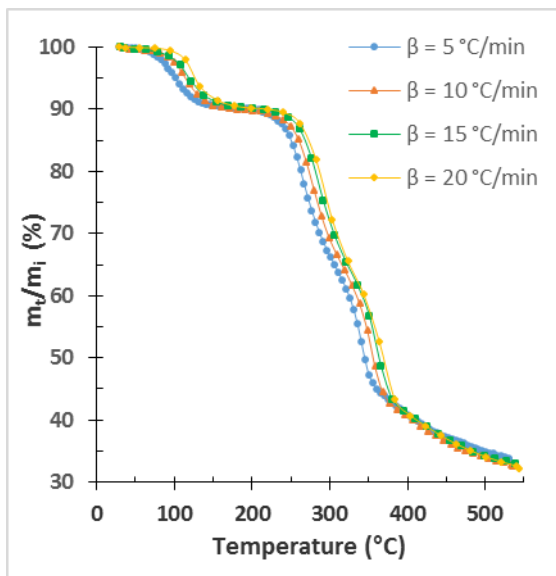


Fig. 1. TG curve of oil-palm shell slow pyrolysis at different heating rates.

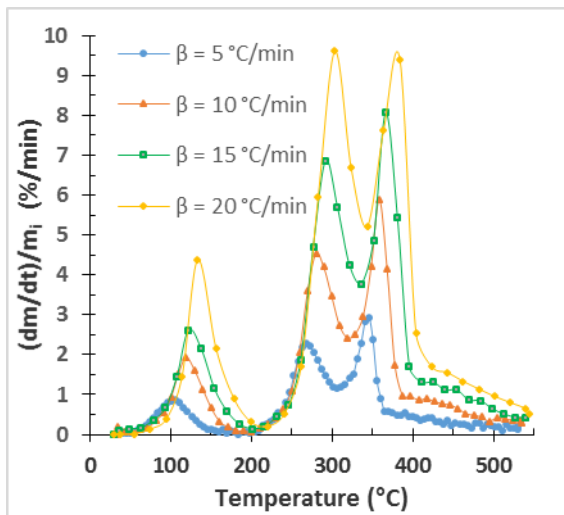


Fig. 2. DTG curve of oil-palm shell slow pyrolysis at different heating rates.

It can be seen that the increase in heating rate shifts the curve consecutively to the higher temperature zone and significantly affects maximum decomposition rate, which tend to increase and be reached at higher temperature. This is in agreement with previous studies [17], [27], [28]. These shifts were possibly caused by the minimum heat required for cracking the particles were reached later at higher temperatures, due to less efficient and less effective heat transfer in faster heating rates [19]. In more detail, the rate

values of maximum mass loss, and the temperatures where those values reached are presented in Table 2.

Table 2. $T_{1,max}$, $T_{2,max}$, $T_{3,max}$ and $(dm/dt)/m_i$ at different heating rates.

β (°C/min)	5	10	15	20
$T_{1,max}$ (°C)	106.02	119.00	121.84	133.37
$(dm/dt)/m_i$ (%/min)	0.87	1.94	2.62	4.39
$T_{2,max}$ (°C)	267.11	279.60	291.66	303.25
$(dm/dt)/m_i$ (%/min)	2.30	4.53	6.87	9.61
$T_{3,max}$ (°C)	345.43	358.08	366.05	383.74
$(dm/dt)/m_i$ (%/min)	2.94	5.88	8.06	9.40

Pyrolysis process commonly comprises: moisture evaporation, main devolatilization and continuous slight devolatilization [29]. This corresponds to this oil-palm shell pyrolysis, where firstly, moisture evaporation with mass loss less than 10 % took place up to 200 °C and maximum decomposition rates which are indicated by the first peaks of curves at Fig. 2, achieved 0.87, 1.94, 2.62 and 4.39 %/min for heating rates of 5, 10, 15, and 20 °C/minute, respectively. Then, followed by main devolatilization stage, that exists in a temperature range of 200 °C - 400 °C. In this active pyrolysis zone, the mass loss of the samples dropped sharply up to 400 °C, as the loss of water and light volatiles compounds took place [30]. Finally, devolatilization continued in the passive pyrolysis zone from 400 °C to 550 °C, by mass loss of slightly greater than 10%.

As has been known that lignocellulosic biomass consists of hemicellulose, cellulose and lignin [7], [24], [31]. There have been some reports on the composition of cellulose, hemicellulose, and lignin for oil-palm shell. Mae et al.[32] reported that oil-palm shell consists of 31 % of cellulose, 20 % of hemicellulose and 49 % of lignin. Meanwhile, Shibata et al.[33] reported that the proportion of cellulose, hemicellulose and lignin in the shell was 20.5 %, 22.3 % and 51.5 %, respectively. So, these indicate that the lignin content was high. It is known that a higher lignin content leads to a slower decomposition with more energy needed, whereas a higher cellulose and hemicellulose content decomposes faster and produces a larger fraction of gaseous products [34].

Based on the previous studies previously conducted, it can be known that each of the components decomposed at different temperature ranges [18], [31], [35]. For example, Vamvuka et al. [18] found that lignin started to decompose at low rate and low temperature of about 200 °C continued until 600 °C. Thus, it decomposed at both active and passive pyrolysis zone. Whereas, hemicellulose decomposed between 200 °C and 350 °C. Then, cellulose is the last component that decomposed at higher temperature range of 280 – 400 °C. These can be described by the fact that cellulose is a semi-crystalline material, while hemicellulose and lignin are non-crystalline ones, so the pyrolysis of

cellulose must first destroy the lattice structure of cellulose which needs extra energy, leading to higher activation energy [22], [36].

By considering the decomposition temperature ranges of to those three components, two peaks of the curves in both active and passive pyrolysis zone in Fig. 2 can be related to the decomposition of hemicellulose, cellulose and lignin. The first peak probably involved hemicellulose and lignin decomposition. While the second peak was formed of cellulose and lignin decomposition.

Maximum peaks were reached at 303.25 °C and 383.74 °C for heating rate of 20 °C/minute. This result has likeness to the studies that have been previously conducted by Slopiecka et al. and Yang et al. [21], [35].

3.2. Effect of heating rate to the kinetic parameters

Based on the thermogravimetric data calculation results, activation energy and frequency factor values at different heating rates can be determined and are shown in Table 3.

Table 3. Activation energy and frequency factor values at different heating rates and reaction order = 1, 2, 3.

(a). at heating rate of 5 °C/min

Temperature range (°C)	Activation energy (kJ/mol)	Frequency factor (s ⁻¹)
$\beta = 5\text{ °C/min, } n = 1$		
355 - 515	9.05	1.283E-01
330 - 355	61.38	2.029E+04
280 - 330	22.06	2.842E+00
245 - 280	52.07	4.591E+03
$\beta = 5\text{ °C/min, } n = 2$		
486 - 525	98.35	1.395E+07
355 - 477	38.89	4.068E+02
330 - 350	114.87	2.707E+09
291 - 326	33.95	7.693E+01
242 - 287	58.93	2.922E+04
$\beta = 5\text{ °C/min, } n = 3$		
481 - 525	194.88	1.598E+15
355 - 477	79.78	6.053E+06
330 - 350	183.96	7.428E+15
306 - 326	55.85	1.812E+04
237 - 301	65.82	1.891E+05

(b). at heating rate of 10 °C/min

Temperature range (°C)	Activation energy (kJ/mol)	Frequency factor (s ⁻¹)
$\beta = 10\text{ °C/min, } n = 1$		
377 - 533	9.46	2.753E-01
338 - 377	55.64	9.268E+03
298 - 338	22.41	5.431E+00
249 - 298	47.61	2.389E+03
$\beta = 10\text{ °C/min, } n = 2$		
503 - 533	97.86	1.984E+07
377 - 494	43.29	1.741E+03
348 - 368	118.48	6.773E+09
308 - 338	36.86	2.505E+02
249 - 299	57.17	2.836E+04
$\beta = 10\text{ °C/min, } n = 3$		
503 - 532	203.10	7.07E+15
387 - 494	92.59	1.03E+08
338 - 337	159.50	5.61E+13
298 - 323	48.02	4.87E+03
259 - 289	77.09	3.69E+06

(c). at heating rate of 15 °C/min

Temperature range (°C)	Activation energy (kJ/mol)	Frequency factor (s ⁻¹)
$\beta = 15\text{ °C/min, } n = 1$		
395 - 539	8.56	3.037E-01
351 - 381	53.84	8.021E+03
306 - 351	25.46	1.565E+01
260 - 306	49.18	4.236E+03
$\beta = 15\text{ °C/min, } n = 2$		
454 - 539	55.17	1.939E+04
395 - 440	34.35	3.745E+02
351 - 381	106.06	6.319E+08
306 - 336	36.70	3.172E+02
260 - 292	61.70	9.771E+04
$\beta = 15\text{ °C/min, } n = 3$		
454 - 539	116.91	7.31E+09
395 - 440	70.22	1.84E+06
351 - 381	174.03	9.31E+14
306 - 336	52.22	1.57E+04
260 - 292	72.72	1.53E+06

(d). at heating rate of 20 °C/min

Temperature range (°C)	Activation energy (kJ/mol)	Frequency factor (s ⁻¹)
$\beta = 20\text{ °C/min, } n = 1$		
403 - 540	6.90	2.321E-01
343 - 403	46.46	2.102E+03
303 - 343	27.36	3.069E+01
261 - 303	49.94	6.054E+03
$\beta = 20\text{ °C/min, } n = 2$		
462 - 540	47.10	4.830E+03
403 - 443	31.29	2.376E+02
343 - 384	87.75	1.912E+07
303 - 343	40.98	1.026E+03
261 - 303	60.06	7.752E+04
$\beta = 20\text{ °C/min, } n = 3$		
442 - 540	95.55	1.76E+08
384 - 423	65.46	8.03E+05
343 - 384	140.96	1.58E+12
303 - 343	57.20	5.61E+04
261 - 303	71.27	1.25E+06

The energy activation and frequency factor values vary according to specific temperature ranges due to the slope difference in a curve at specific heating rate and reaction orders. At reaction order of one, the values of energy activation and frequency factor can be approximated by four temperature ranges, while at both reaction order of two and three, by five temperature ranges. The heating rate increase shifted the temperature ranges into higher temperature values for the corresponding ranges. The activation energy values are from 6.90 to 203.10 kJ/mol and frequency factor values range from 1.283E-01 to 7.07E+15 s⁻¹.

Moreover, It can also be seen that the activation energy and frequency factor increase with the increase of reaction order. This is possibly caused by different chemical structures among cellulose, hemicellulose and lignin which may affect their activation energies. Furthermore, Amorphous nature of hemicellulose cause it to be less stable than two others. Due to its strong inter-molecular hydrogen bonding, cellulose required higher activation energy than hemicellulose. Whereas, complex structure with many oxygenated functional groups, and the scission of the associated bonds in lignin which can occur in different temperature ranges cause various thermal stability in lignin [37].

It appears at Fig.3 that for all heating rates applied, the second order reaction gives generally a best representation of the main pyrolysis process with the correlation coefficient, R², around 0.99, eventhough at heating rate of 20 °C/min, the second and third order reaction have the same correlation coefficient.

4. Conclusions

Heating rate affects the thermogravimetric curve position, maximum decomposition rate and maximum temperature where maximum loss rate took place.

The activation energy and frequency factor values vary according to the specific temperature ranges due to the slope difference in a curve at specific heating rate and reaction order.

Accordingly, the pyrolysis stages were approximately divided into four temperature ranges for reaction order of one and into five ones for reaction order of two and three, so that the activation energy values obtained are from 6.90 to 203.10 kJ/mol and frequency factor values range from 1.283E-01 to 7.07E+15 s⁻¹.

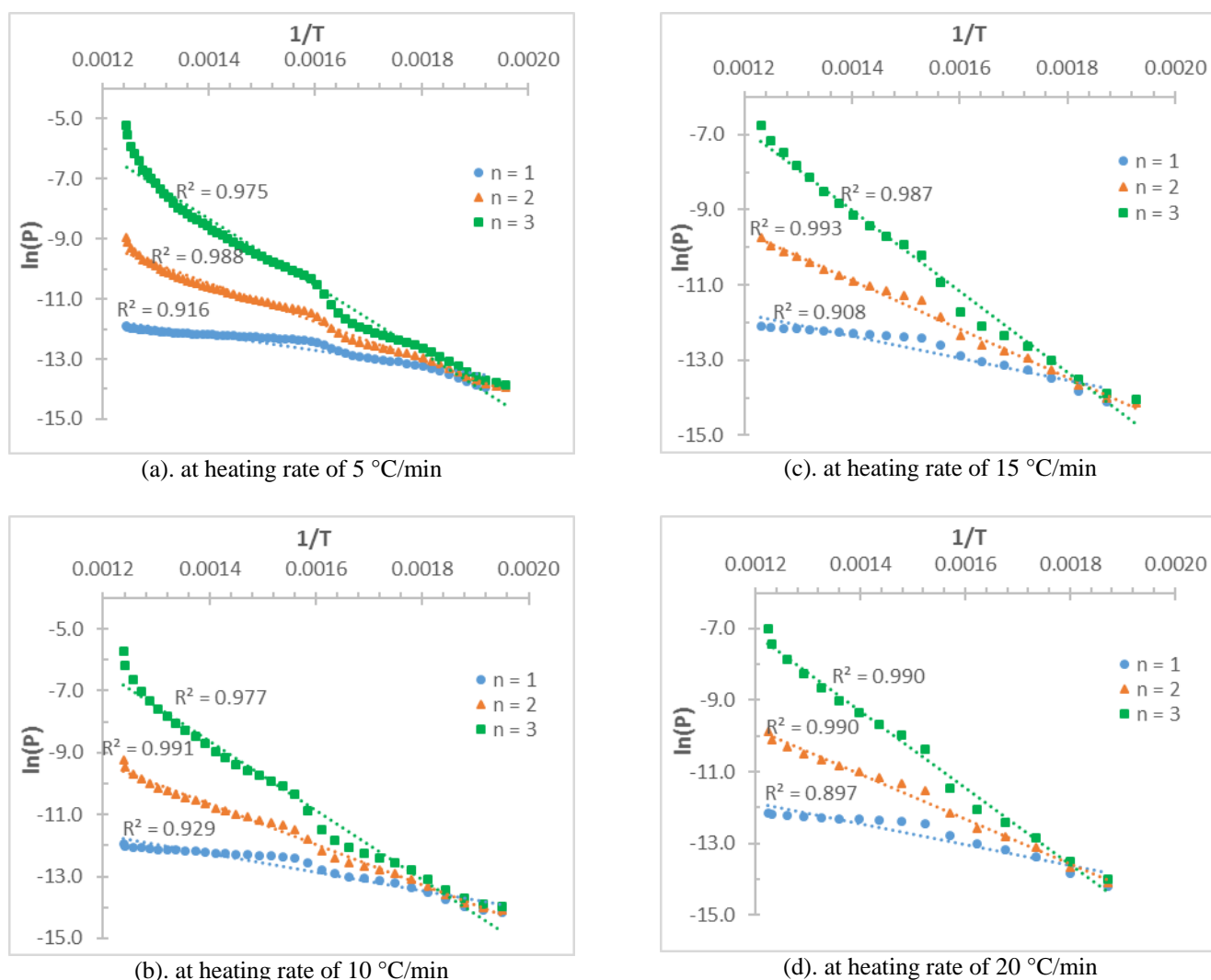


Fig. 3. Plots of ln(P) versus 1/T at different heating rates ; $P = \ln\{[-\ln(1-\alpha)]/T^2\}$ for $n = 1$ and $P = [(1-(1-\alpha)^{1-n})]/((1-n)T^2)$ for $n = 2$ and $n = 3$

The temperature ranges tend to shift into higher temperature values with heating rate increase at the corresponding ranges, and for all heating rates applied, the second order reaction gives generally a best representation of the main pyrolysis process.

Acknowledgements

The authors acknowledge gratefully to Mr. Sudarto from Institute of Plantation Education, Yogyakarta for supplying oil-palm shells and the Ministry of Research, Technology and Higher Education – Republic of Indonesia for financial support.

References

- [1] A. Z. Aktas, "A Review and Comparison of Renewable Energy Strategies or Policies of Some Countries," in *International Conference on Renewable Energy Research and Applications*, 2015, pp. 636–643.
- [2] L. J. R. Nunes, J. C. O. Matias, and J. P. S. Catalão, "Application of Biomass for the Production of Energy in the Portuguese Textile Industry," in *International Conference on Renewable Energy Research and Applications*, 2013, pp. 336–341.
- [3] M. Oku, N. Hayashi, T. Sakoda, and D. Tashima, "Basic Characteristics of a Heat and Electricity Combined Generation System Using Biomass Fuel," in *International Conference on Renewable Energy Research and Applications*, 2014, pp. 222–228.
- [4] N. S. Kee, *The Oil Palm, its Culture, Manuring and Utilisation*. International Potash Institute, 1972.
- [5] U. S. D. of A. Foreign Agriculture Service, "World's Palm Oil Production," 2007.
- [6] S. H. Chang, "An overview of empty fruit bunch from oil palm as feedstock for bio-oil production," *Biomass and Bioenergy*, vol. 62, pp. 174–181, 2014.
- [7] H. V. Ly, J. Kim, and S. Kim, "Pyrolysis characteristics and kinetics of palm fiber in a closed reactor," *Renew. Energy*, vol. 54, pp. 91–95, 2013.
- [8] P. Mckendry, "Energy production from biomass (part 2)," *Bioresour. Technol.*, vol. 83, pp. 47–54, 2002.
- [9] E. Okoroigwe, "Combustion Analysis and Devolatilization kinetics of Gmelina, Mango, Neem and Tropical Almond Woods under Oxidative Condition," *Int. J. Renew. Energy Res.*, vol. 5, no. 4, pp. 1024–1033, 2015.
- [10] M. S. Kumar, A. Singh, J. V.P., R. A. Murali, A. Revuru, and A. Das, "Thermodynamic Analysis of Torrefaction Process," *Int. J. Renew. Energy Res.*, vol. 6, no. 1, pp. 245–249, 2016.
- [11] M. M. Said, G. R. John, and C. F. Mhilu, "Thermal Characteristics And Kinetics Of Rice Husk For Pyrolysis Process," *Int. J. Renew. Energy Res.*, vol. 4, no. 2, pp. 275–278, 2014.
- [12] Y. I. Tosun, "The Proposed Design of Co-Combustion Stoker for Sirnak Agricultural Biomass Waste and Sirnak Asphaltite in 35 MW Electricity Production," in *International Conference on Renewable Energy Research and Applications*, 2015, pp. 358–363.
- [13] S. Ceylan and D. Kazan, "Bioresource Technology Pyrolysis kinetics and thermal characteristics of microalgae *Nannochloropsis oculata* and *Tetraselmis* sp.," *Bioresour. Technol.*, vol. 187, pp. 1–5, 2015.
- [14] M. Poletto, A. J. Zattera, and R. M. C. Santana, "Thermal decomposition of wood: Kinetics and degradation mechanisms," *Bioresour. Technol.*, vol. 126, pp. 7–12, 2012.
- [15] S. Hosokai, K. Matsuoka, K. Kuramoto, and Y. Suzuki, "Estimation of thermodynamic properties of liquid fuel from biomass pyrolysis," in *International Conference on Renewable Energy Research and Applications*, 2014, pp. 728–731.
- [16] S. A. El-Sayed and M. E. Mostafa, "Pyrolysis characteristics and kinetic parameters determination of biomass fuel powders by differential thermal gravimetric analysis (TGA/DTG)," *Energy Convers. Manag.*, vol. 85, pp. 165–172, 2014.
- [17] C. Gai, Y. Dong, and T. Zhang, "The kinetic analysis of the pyrolysis of agricultural residue under non-isothermal conditions," *Bioresour. Technol.*, vol. 127, pp. 298–305, 2013.
- [18] D. Vamvuka and S. Sfakiotakis, "Effects of heating rate and water leaching of perennial energy crops on pyrolysis characteristics and kinetics," *Renew. Energy*, vol. 36, pp. 2433–2439, 2011.
- [19] T. Mani, P. Murugan, J. Abedi, and N. Mahinpey, "Pyrolysis of wheat straw in a thermogravimetric analyzer: Effect of particle size and heating rate on devolatilization and estimation of global kinetics," *Chem. Eng. Res. Des.*, vol. 88, pp. 952–958, 2010.
- [20] J. E. White, W. J. Catallo, and B. L. Legendre, "Biomass pyrolysis kinetics: a comparative critical review with relevant agricultural residue case studies," *J. Anal. Appl. Pyrolysis*, vol. 91, pp. 1–33, 2011.
- [21] K. Slopicka, P. Bartocci, and F. Fantozzi, "Thermogravimetric analysis and kinetic study of poplar wood pyrolysis," *Appl. Energy*, vol. 97, pp. 491–497, 2012.
- [22] D. Chen, J. Zhou, and Q. Zhang, "Effects of heating rate on slow pyrolysis behavior, kinetic parameters and products properties of moso bamboo," *Bioresour. Technol.*, vol. 169, pp. 313–319, 2014.
- [23] S. Ceylan and Y. Topçu, "Bioresource Technology Pyrolysis kinetics of hazelnut husk using thermogravimetric analysis," *Bioresour. Technol.*, vol. 156, pp. 182–188, 2014.

- [24] U. Ozveren and Z. S. Ozdogan, "Investigation of the slow pyrolysis kinetics of olive oil pomace using thermo-gravimetric analysis coupled with mass spectrometry," *Biomass and Bioenergy*, vol. 58, pp. 168–179, 2013.
- [25] H. H. Sait, A. Hussain, A. A. Salema, and F. N. Ani, "Pyrolysis and combustion kinetics of date palm biomass using thermogravimetric analysis," *Bioresour. Technol.*, vol. 118, pp. 382–389, 2012.
- [26] A. Kumar, L. Wang, Y. A. Dzenis, D. D. Jones, and M. A. Hanna, "Thermogravimetric characterization of corn stover as gasification and pyrolysis feedstock," *Biomass and Bioenergy*, vol. 32, pp. 460–467, 2008.
- [27] S. Ceylan, Y. Topcu, and Z. Ceylan, "Thermal behaviour and kinetics of alga *Polysiphonia elongata* biomass during pyrolysis," *Bioresour. Technol.*, vol. 171, pp. 193–198, 2014.
- [28] G. Wang, W. Li, B. Li, and H. Chen, "TG study on pyrolysis of biomass and its three components under syngas q," vol. 87, pp. 552–558, 2008.
- [29] G. Mishra and T. Bhaskar, "Non isothermal model free kinetics for pyrolysis of rice straw," *Bioresour. Technol.*, vol. 169, pp. 614–621, 2014.
- [30] M. Jeguirim and G. Trouvé, "Pyrolysis characteristics and kinetics of *Arundo donax* using thermogravimetric analysis," *Bioresour. Technol.*, vol. 100, pp. 4026–4031, 2009.
- [31] G. Dorez, L. Ferry, R. Sonnier, and A. Taguet, "Effect of cellulose, hemicellulose and lignin contents on pyrolysis and combustion of natural fibers," *J. Anal. Appl. Pyrolysis*, vol. 107, pp. 323–331, 2014.
- [32] K. Mae, I. Hasegawa, N. Sakai, and K. Miura, "A New Conversion Method for Recovering Valuable Chemicals from Oil Palm Shell Wastes Utilizing Liquid-Phase Oxidation with H₂O₂ under Mild Conditions," vol. 35, no. 1, pp. 1212–1218, 2000.
- [33] M. Shibata, M. Varman, Y. Tono, H. Miyafuji, and S. Saka, "Characterization in Chemical Composition of the Oil Palm (*Elaeis guineensis*)," *J. Japan Energy Inst.*, vol. 87, pp. 383–388, 2008.
- [34] L. Burhenne, J. Messmer, T. Aicher, and M.-P. Laborie, "The effect of the biomass components lignin, cellulose and hemicellulose on TGA and fixed bed pyrolysis," *J. Anal. Appl. Pyrolysis*, vol. 101, pp. 177–184, 2013.
- [35] H. Yang, R. Yan, H. Chen, D. H. Lee, and C. Zheng, "Characteristics of hemicellulose, cellulose and lignin pyrolysis," *Fuel*, vol. 86, no. 12–13, pp. 1781–1788, 2007.
- [36] G. Jiang, D. J. Nowakowski, and A. V Bridgwater, "A systematic study of the kinetics of lignin pyrolysis," *Thermochim. Acta*, vol. 498, pp. 61–66, 2010.
- [37] V. Pasangulapati, K. D. Ramachandriya, A. Kumar, M. R. Wilkins, C. L. Jones, and R. L. Huhnke, "Effects of cellulose, hemicellulose and lignin on thermochemical conversion characteristics of the selected biomass," *Bioresour. Technol.*, vol. 114, pp. 663–669, 2012.